



OPEN

A nickel phosphide nanoalloy catalyst for the C-3 alkylation of oxindoles with alcohols

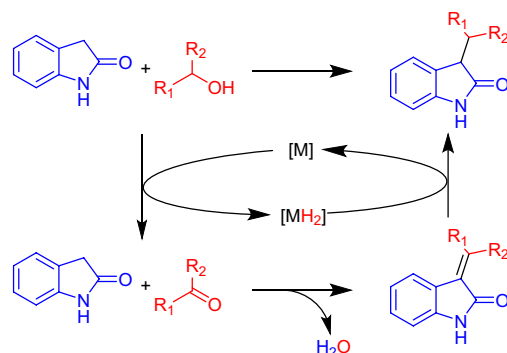
Shu Fujita¹, Kohei Imagawa¹, Sho Yamaguchi¹, Jun Yamasaki², Seiji Yamazoe³, Tomoo Mizugaki^{1,4} & Takato Mitsudome¹✉

Although transition metal phosphides are well studied as electrocatalysts and hydrotreating catalysts, the application of metal phosphides in organic synthesis is rare, and cooperative catalysis between metal phosphides and supports remains unexplored. Herein, we report that a cerium dioxide-supported nickel phosphide nanoalloy (nano-Ni₂P/CeO₂) efficiently promoted the C-3 alkylation of oxindoles with alcohols without any additives through the borrowing hydrogen methodology. Oxindoles were alkylated with various alcohols to provide the corresponding C-3 alkylated oxindoles in high yields. This is the first catalytic system for the C-3 alkylation of oxindoles with alcohols using a non-precious metal-based heterogeneous catalyst. The catalytic activity of nano-Ni₂P/CeO₂ was comparable to that reported for precious metal-based catalysts. Moreover, nano-Ni₂P/CeO₂ was easily recoverable and reusable without any significant loss of activity. Control experiments revealed that the Ni₂P nanoalloy and the CeO₂ support functioned cooperatively, leading to a high catalytic performance.

Metal–metal nanoalloys have been recognized as key materials for the development of novel catalysts. In contrast, metal–nonmetal nanoalloys have not been widely studied in the field of fine chemical synthesis. In this context, metal phosphides have recently received growing attention as electrocatalysts for the hydrogen evolution reaction^{1–3} and hydrodesulfurization catalysts in the petroleum industry^{4–6} due to the fact that they exhibit unique catalysis derived from the charge transfer effect of metal to phosphorus^{7,8} and the ensemble effect^{9,10}. Despite these fascinating properties, the application of metal phosphides in liquid-phase organic synthesis is rare^{11–19}, with the majority of reported reactions to date being simple hydrogenation reactions^{20–47}. Therefore, the study of metal phosphide catalysis for organic synthesis remains an exciting and unexplored research area. Furthermore, although supports are known to greatly improve catalytic performances, cooperative catalysis between metal phosphides and supports has yet to be comprehensively explored. Therefore, functionalization by combining a support and a metal phosphide catalyst is expected to lead to new metal phosphide catalysts for other organic transformations.

The C-3 alkylation of oxindoles is one of the key routes to the synthesis of functionalized oxindoles that possess significant potential for use in a wide range of biological applications, including as NMDA antagonists⁴⁸, antiangiogenic agents⁴⁹, and anti-cancer drugs⁵⁰. Recently, catalytic methods using alcohols as alkylating reagents have attracted attention for the C-3 alkylation of oxindoles because this reaction proceeds through the borrowing hydrogen (BH) methodology with the co-production of only water, thereby providing a high atom efficiency (Scheme 1)⁵¹. In addition, various metal complex catalysts have been reported for the alkylation reaction with alcohols^{50–63}. However, these catalysts inevitably require complex ligands and the addition of strong bases. Furthermore, difficulties in the separation and reuse of these catalysts remain an ongoing issue. As an alternative, reusable heterogeneous catalysts based on precious metals have been developed for the C-3 alkylation reaction^{64–66}. Although these catalysts are effective, they are both expensive and rare. In terms of non-precious metal-based heterogeneous catalysts, only Raney Ni has been reported to date^{67,68}. However, a large amount of Ni is required to promote the alkylation, and the turnover number (TON) tends to be low (i.e., <0.6), thereby indicating that this system possesses an inadequate catalytic efficiency. Therefore, the development of highly

¹Department of Materials Engineering Science, Graduate School of Engineering Science, Osaka University, 1-3 Machikaneyama, Toyonaka, Osaka 560-8531, Japan. ²Research Center for Ultra-High Voltage Electron Microscopy, Osaka University, 7-1, Mihogaoka, Ibaraki, Osaka 567-0047, Japan. ³Department of Chemistry, Tokyo Metropolitan University, 1-1 Minami Osawa, Hachioji, Tokyo 192-0397, Japan. ⁴Innovative Catalysis Science Division, Institute for Open and Transdisciplinary Research Initiatives (ICS-OTRI), Osaka University, Suita, Osaka 565-0871, Japan. ✉email: mitsudome@cheng.es.osaka-u.ac.jp



Scheme 1. C-3 alkylation of oxindole with alcohols through the borrowing hydrogen methodology.

active and reusable non-precious metal-based catalysts for the C-3 alkylation of oxindoles with alcohols remains a great challenge.

We herein report the preparation and application of a cerium dioxide-supported nickel phosphide nanoalloy (nano-Ni₂P/CeO₂) for the synthesis of C-3 functionalized oxindoles using alcohols through the BH methodology without the need for additives. This constitutes the first catalytic system for the synthesis of C-3 functionalized oxindoles using a non-precious metal-based heterogeneous catalyst. Furthermore, the recovery and reuse of nano-Ni₂P/CeO₂ are also evaluated.

Results and discussion

The desired nano-Ni₂P was prepared according to our previous report with some modifications (see Supplementary Information for details)⁴³. More specifically, NiCl₂·6H₂O was added to hexadecylamine in the presence of triphenylphosphite. The mixture was heated at 120 °C in vacuo, and then the temperature was increased to 320 °C under Ar atmosphere. The precipitate was collected by centrifugation and washed with acetone and chloroform to afford the nano-Ni₂P. Subsequently, this nano-Ni₂P was dispersed in hexane and stirred with CeO₂, yielding the desired nano-Ni₂P/CeO₂ (Fig. S1). BET surface area of the transmission electron microscopy (TEM) images of the nano-Ni₂P/support catalysts are shown in Table S1 and Fig. S2, respectively. The formation of nano-Ni₂P was confirmed by X-ray diffraction (XRD) measurements, whereby the diffraction peaks located at 2θ = 40.8, 44.7, 47.3, and 54.1° were attributed to the (111), (201), (210), and (300) planes of Ni₂P (JCPDS card no. 03-0953), respectively (Fig. S3). A representative TEM image of nano-Ni₂P revealed a collection of spherical nanoparticles with a mean diameter of 5.4 nm (Fig. 1a). The elemental distributions of Ni and P on CeO₂ were determined using high-angle annular dark field scanning transmission electron microscopy (HAADF-STEM) coupled with energy dispersive X-ray spectroscopy (EDX; Fig. 1b–f). It was found that nano-Ni₂P was highly dispersed on the CeO₂ support, in which Ni and P were homogeneously distributed. These results demonstrate that nano-Ni₂P is uniformly immobilized on the surface of CeO₂. Furthermore, the Ni *K*-edge X-ray absorption near edge structure (XANES) spectrum shows that the absorption edge energy of nano-Ni₂P/CeO₂ is close to that of Ni foil, suggesting that the Ni species in nano-Ni₂P/CeO₂ possesses metallic states (Fig. S4). This conclusion is also supported by the result of the XPS analysis of nano-Ni₂P/CeO₂, where two peaks observed at 852.7 and 869.9 eV are similar to those of metallic Ni 2p_{3/2} (852.8 eV) and Ni 2p_{1/2} (870.0 eV), respectively (Fig. S5).

Initially, the catalytic potential of the nano-Ni₂P/support catalysts for the C-3 alkylation of oxindole with benzyl alcohol was investigated at 140 °C for 10 h in toluene (Table 1). Notably, nano-Ni₂P/CeO₂ exhibited a high catalytic activity to provide 3-benzyl-2-oxindole (**1a**) in 95% yield (entry 1). In contrast, nano-Ni₂P/TiO₂ and nano-Ni₂P/SiO₂ gave low yields of **1a**, accompanied by the production of 3-benzylideneoxindole (**2a**) in ca. 30% yield (entries 2 and 3). Furthermore, nano-Ni₂P immobilized on other supports such as Al₂O₃, hydrotalcite (HT, Mg₆Al₂(OH)₁₆CO₃·4H₂O), MgO, Nb₂O₅, and ZnO showed almost no activity for the C-3 alkylation of oxindole (entries 4–8), indicating that modulation of the support significantly affects the catalytic performance of nano-Ni₂P for the alkylation reaction. For comparison with nano-Ni₂P/CeO₂, Ni/CeO₂ was prepared via the impregnation method, and H₂-treated Ni/CeO₂ (Ni/CeO₂-Red) was also synthesized. These species were subjected to testing as model catalysts for the conventional Ni nanoparticles of NiO and Ni(0), respectively, in the C-3 alkylation of oxindole with benzyl alcohol (see Supplementary Information for details regarding catalyst preparation). However, in sharp contrast to the highly active nano-Ni₂P/CeO₂, these conventional nickel nanoparticle catalysts exhibited very low activities (entries 9 and 10). These results clearly demonstrate the importance of the combination of nano-Ni₂P with a CeO₂ support for efficiently promoting the alkylation of oxindole.

With the nano-Ni₂P/CeO₂ in hand, we explored the substrate scope in the C-3 alkylation of oxindoles with alcohols (Scheme 2). Benzyl alcohols substituted with electron-withdrawing or electron-donating groups, such as methyl, halogen, trifluoromethyl, methoxy, and phenyl groups, were reacted with oxindole to afford the corresponding mono-C-3 alkylated oxindoles in high yields (**1a–1j**). It was also found that nano-Ni₂P/CeO₂ promoted the C-3 alkylation of oxindole with heterocyclic alcohols, such as 2-thiophenemethanol and 4-pyridinemethanol, although nitrogen or sulfur atoms often coordinate strongly to the metals, resulting in catalyst deactivation (**1k** and **1l**)^{69,70}. Furfuryl alcohol, which is an important biomass-derived chemical alternative to petroleum-based chemicals, also acted as a good alkylation reagent to provide the corresponding C-3

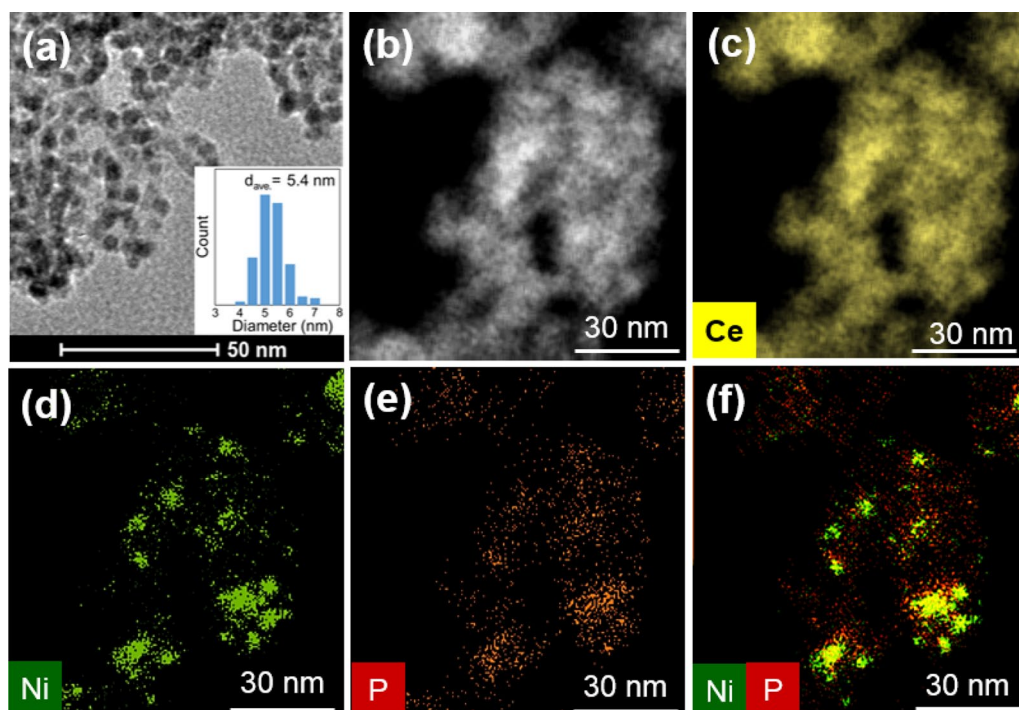
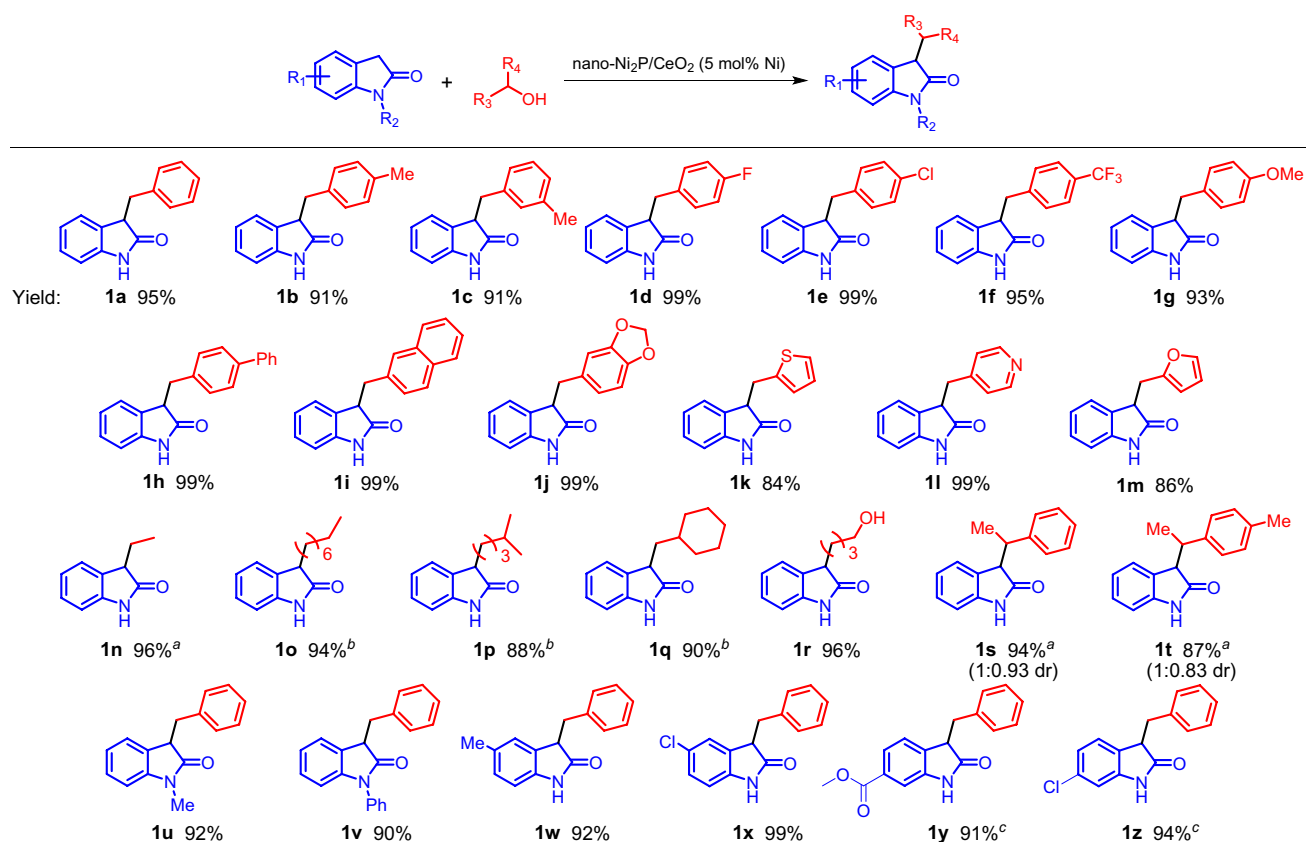


Figure 1. (a) TEM image of nano-Ni₂P (the inset shows the histogram of nano-Ni₂P). (b) HAADF-STEM image of nano-Ni₂P/CeO₂. Elemental mapping of (c) Ce, (d) Ni, and (e) P, and (f) a composite overlay of (d,e).

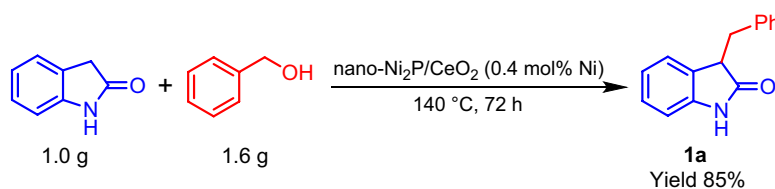
Entry	Catalyst	Conv. (%)	Yield (%) ^b	
			1a	2a
1	Nano-Ni ₂ P/CeO ₂	>99	95	4
2	Nano-Ni ₂ P/TiO ₂	51	12	26
3	Nano-Ni ₂ P/SiO ₂	33	3	29
4	Nano-Ni ₂ P/Al ₂ O ₃	3	1	1
5	Nano-Ni ₂ P/HT	3	0	1
6	Nano-Ni ₂ P/MgO	2	0	0
7	Nano-Ni ₂ P/Nb ₂ O ₅	5	0	0
8	Nano-Ni ₂ P/ZnO	4	0	0
9	Ni/CeO ₂	30	14	10
10	Ni/CeO ₂ -Red	9	6	3

Table 1. C-3 alkylation of oxindole with benzyl alcohol using Ni catalysts^a. ^aReaction conditions: catalyst (0.15 g, 5 mol% Ni), oxindole (0.5 mmol), benzyl alcohol (1 mmol), toluene (2 mL), 140 °C, 10 h, N₂ atmosphere. ^bYields based on oxindole were determined by gas chromatography-mass spectrometry (GC-MS) using naphthalene as an internal standard.

alkylated oxindole (**1m**)⁷¹. Less active aliphatic alcohols (**1n–1r**) and secondary alcohols (**1s** and **1t**) could be applied to this catalytic system, giving the corresponding products in high yields. Notably, when 1,4-butanediol was used as the alkylating agent, mono-C3-alkylated oxindole was selectively obtained without the formation of di-alkylated products (**1r**). The excellent performance of nano-Ni₂P/CeO₂ was also demonstrated in the C-3 alkylation using 1-phenylethanol and 1-(*p*-tolyl)ethanol, which are challenging reagents due to their steric



Scheme 2. Substrate scope of the C-3 alkylation of oxindoles with alcohols catalyzed by nano-Ni₂P/CeO₂. Reaction conditions: nano-Ni₂P/CeO₂ (0.15 g, 5 mol% Ni), oxindole (0.5 mmol), alcohol (1 mmol), toluene (2 mL), 140 °C, 10 h, N₂ atmosphere. Yields based on oxindole were determined by GC–MS using naphthalene as an internal standard. ^aAlcohol (5 mmol), 180 °C, 24 h. ^bAlcohol (5 mmol), 160 °C, 24 h. ^c160 °C, 24 h.



Scheme 3. The gram-scale C-3 alkylation of oxindole with benzyl alcohol catalyzed by nano-Ni₂P/CeO₂. Reaction conditions: nano-Ni₂P/CeO₂ (0.4 mol% Ni), oxindole (1.0 g; 7.5 mmol), benzyl alcohol (1.6 g; 15 mmol), 140 °C, 72 h, N₂ atmosphere. The yield based on oxindole was determined by GC–MS using naphthalene as an internal standard.

hindrances (**1s** and **1t**)⁶¹. Various oxindoles such as 1-methyloxindole, 1-phenyloxindole, 5-methyloxindole, 5-chlorooxindole, methyl-2-oxindole-6-carboxylate, and 6-chlorooxindole, were also alkylated with benzyl alcohol to provide the desired products in >90% yields (**1u–1z**). The above results therefore demonstrate that nano-Ni₂P/CeO₂ functions as a highly active catalyst for the C-3 alkylation of oxindoles with a wide range of alcohols.

Furthermore, Ni₂P/CeO₂ was found to be applicable to a gram-scale reaction, with 1.0 g of oxindole being converted into **1a** in 85% yield, where the TON reached 212 (Scheme 3). This TON is greater than those of previously reported precious metal-based heterogeneous catalyst systems (Table S2), indicating the high performance of nano-Ni₂P/CeO₂ compared to those of the precious metal catalysts.

Subsequently, the durability of nano-Ni₂P/CeO₂ was assessed through recycling experiments. After the alkylation of oxindole with benzyl alcohol, nano-Ni₂P/CeO₂ was easily recovered from the reaction mixture by centrifugation, and was used again in the following run without any pre-treatment (Fig. 2). Indeed, nano-Ni₂P/CeO₂ provided a high yield of **1a** even after the 6th recycling experiment. We further investigated the reaction rate at an incomplete reaction time (4 h), and found that **1a** (open diamond in Fig. 2) was obtained in similar yields using reused and fresh nano-Ni₂P/CeO₂, thereby demonstrating the excellent reusability of this catalyst.

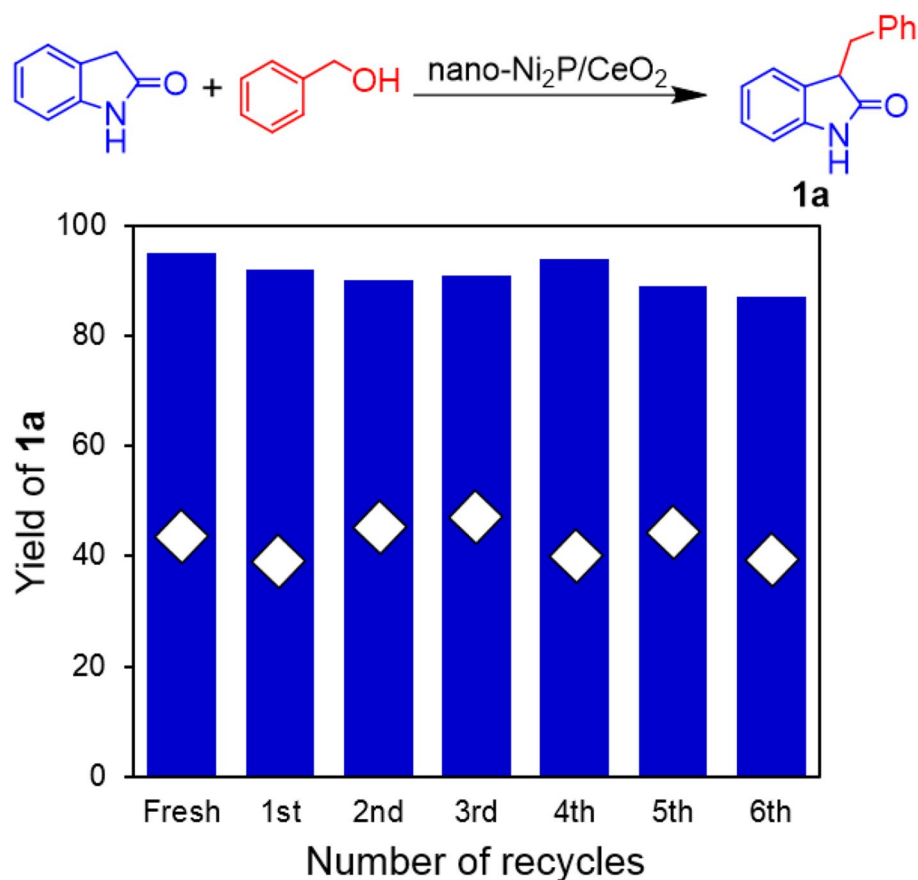


Figure 2. Nano- $\text{Ni}_2\text{P}/\text{CeO}_2$ recycling experiments for the C-3 alkylation of oxindole with benzyl alcohol. Reaction conditions: nano- $\text{Ni}_2\text{P}/\text{CeO}_2$ (0.15 g; 5 mol% Ni), oxindole (0.5 mmol), benzyl alcohol (1 mmol), toluene (2 mL), 140 °C, N_2 atmosphere. Reaction time: 10 h (blue bars), 4 h (open diamond). Yields based on oxindole were determined by GC-MS using naphthalene as an internal standard.

Inductively coupled plasma atomic emission spectrometry (ICP-AES) analysis revealed that the concentration of Ni in the solution after the alkylation was below the detection limit (0.1 ppm), and elemental analysis of the nano- $\text{Ni}_2\text{P}/\text{CeO}_2$ showed that the Ni content of catalyst did not change following the reaction (Table S3). These results clearly demonstrate the high durability of nano- $\text{Ni}_2\text{P}/\text{CeO}_2$ in the C-3 alkylation reactions of oxindole.

Figure 3 shows the time profile of the C-3 alkylation of oxindole with benzyl alcohol catalyzed by nano- $\text{Ni}_2\text{P}/\text{CeO}_2$. During the first 4 h, oxindole was rapidly consumed, accompanied by the formation of **2a**. Afterwards, the yield of **2a** gradually decreased with an increase in the yield of **1a**. These results indicate that **2a** is an intermediate in the C-3 alkylation of oxindole with benzyl alcohol. To clarify the roles of nano- Ni_2P and CeO_2 in the C-3 alkylation of oxindole using alcohols, control experiments were conducted, as outlined in Fig. 4. Initially, a reaction using oxindole and benzyl alcohol was carried out in the presence of nano- Ni_2P , CeO_2 , or nano- $\text{Ni}_2\text{P}/\text{CeO}_2$ under the same reaction conditions as presented in Table 1, with the exception that a shorter reaction time was employed (i.e., 3 h) (Fig. 4a). As shown, nano- $\text{Ni}_2\text{P}/\text{CeO}_2$ promoted the reaction, giving **1a** and **2a** in 20 and 60% yields, respectively. On the other hand, nano- Ni_2P yielded a trace of the desired product **1a**, and reaction intermediate **2a** was formed in 14% yield. When CeO_2 was used, the reaction produced only small amounts of **1a** and **2a**. Subsequently, the condensation of oxindole with benzaldehyde was carried out using nano- Ni_2P or CeO_2 (Fig. 4b). When either nano- Ni_2P or CeO_2 was used, the aldol-type condensation proceeded efficiently to provide **2a** in a high yield. In a blank test, no formation of **2a** was observed, indicating that nano- Ni_2P and CeO_2 are active for the condensation reaction. The above results demonstrate that benzaldehyde is produced on nano- Ni_2P by the dehydrogenation of benzyl alcohol, and subsequently, the aldol-type condensation of benzaldehyde with oxindole occurs on either nano- Ni_2P or CeO_2 ⁷². It is therefore considered that the hydrogen generated on nano- Ni_2P during dehydrogenation may spill over onto the CeO_2 surface, thereby allowing the hydrogenation of **2a** to **1a** on CeO_2 ^{73,74}. Indeed, hydrogen spillover on metal nanoparticle-supported CeO_2 and hydrogen transfer catalysis by CeO_2 have both been reported^{75,76}. Considering the above information, we proposed a reaction pathway for the C-3 alkylation of oxindole with alcohol catalyzed by nano- $\text{Ni}_2\text{P}/\text{CeO}_2$ using the BH methodology (Scheme 4). Initially, the alcohol is dehydrogenated to the corresponding carbonyl compound by nano- Ni_2P (I). The hydrogen generated on the nano- Ni_2P then spills over onto the CeO_2 surface (II), and the aldol-type condensation of oxindole with the carbonyl compound occurs catalyzed by either nano- Ni_2P or CeO_2 to provide an

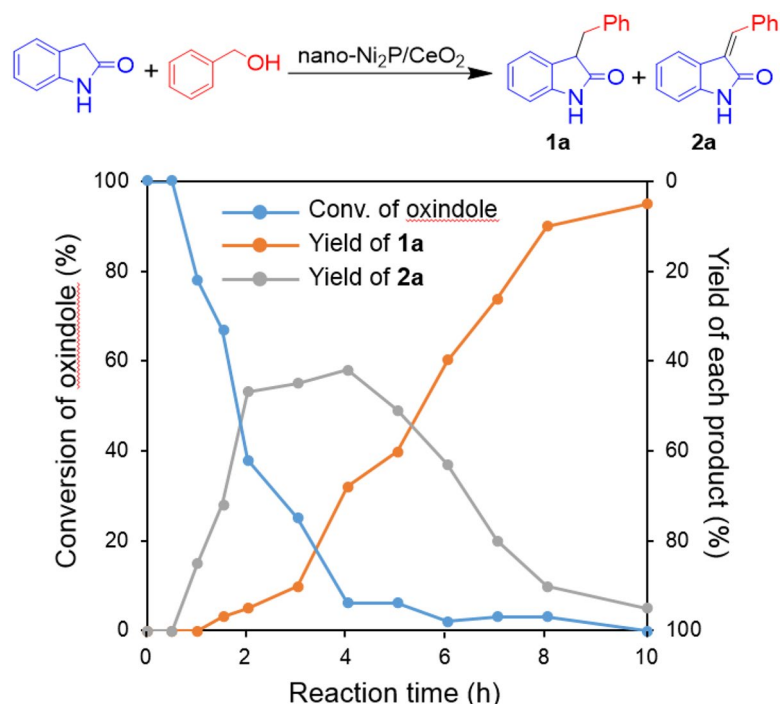


Figure 3. Reaction profile for the C-3 alkylation of oxindole with benzyl alcohol catalyzed by nano-Ni₂P/CeO₂. Reaction conditions: nano-Ni₂P/CeO₂ (5 mol% Ni), oxindole (0.5 mmol), benzyl alcohol (1 mmol), toluene (2 mL), 140 °C, N₂ atmosphere. The conversions and yields were calculated based on oxindole.

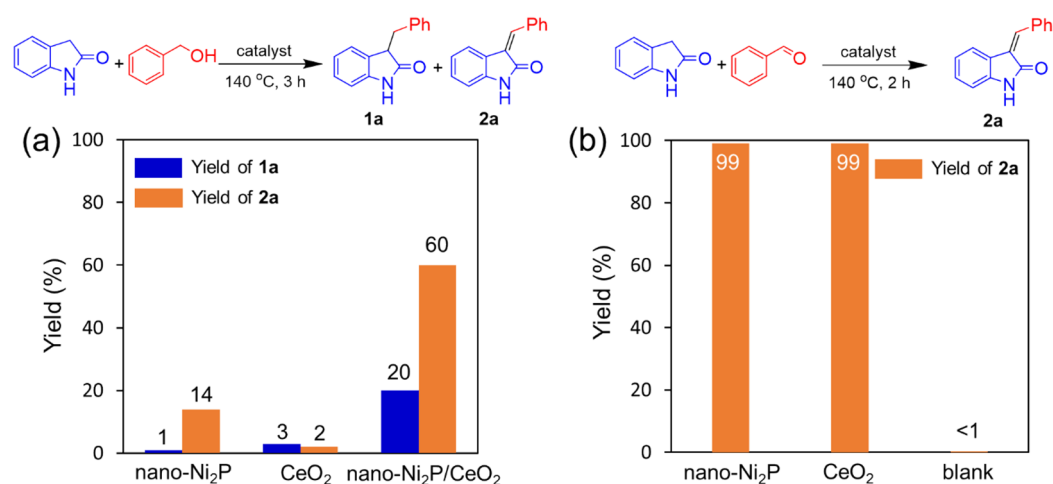
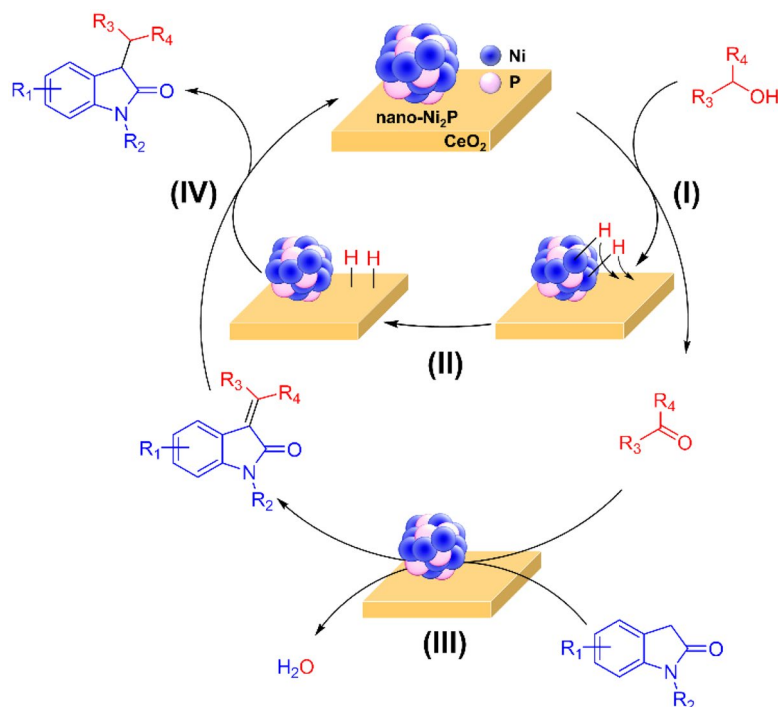


Figure 4. Control experiments for (a) the C-3 alkylation of oxindole with benzyl alcohol, and (b) the aldol-type condensation of oxindole with benzaldehyde. Reaction conditions: nano-Ni₂P (4.3 mg), CeO₂ or nano-Ni₂P/CeO₂ (0.15 g), oxindole (0.5 mmol), benzyl alcohol or benzaldehyde (1 mmol), toluene (2 mL), N₂ atmosphere. Yields based on oxindole were determined by GC-MS using naphthalene as an internal standard.

alkenyloxindole intermediate (III). Finally, the subsequent hydrogenation of alkenyloxindole following hydrogen spillover to CeO₂ yields the desired C3-alkylated product (IV). This well-designed cooperative catalysis by nano-Ni₂P and CeO₂ is a key factor in efficiently promoting the C-3 alkylation of oxindole using alcohols.

Conclusions

We herein report the development of a highly efficient and reusable non-precious metal-based heterogeneous catalyst for promoting the C-3 alkylation of oxindoles with alcohols. More specifically, a cerium dioxide-supported nickel phosphide nanoalloy (nano-Ni₂P/CeO₂) catalyst efficiently promoted the C-3 alkylation of oxindoles with alcohols. This catalytic system was applicable to various alcohols, including benzylic and aliphatic



Scheme 4. Proposed reaction pathway for the C-3 alkylation of oxindoles with alcohols catalyzed by nano-Ni₂P/CeO₂.

alcohols, providing the corresponding products in high yields. Indeed, this is the first catalytic system for the C-3 alkylation of oxindoles with alcohols using non-precious metal-based heterogeneous catalysts. Furthermore, nano-Ni₂P/CeO₂ was easily recoverable and reusable without any significant loss in activity. The catalytic activity of nano-Ni₂P/CeO₂ was high, and was comparable to those of previously reported precious metal-based catalysts. In this reaction, the cooperation between nano-Ni₂P and CeO₂ was found to play a key role; nano-Ni₂P dehydrogenates the alcohol to generate the corresponding carbonyl compound and hydrogen. Subsequently, nano-Ni₂P or CeO₂ promotes the aldol condensation of oxindoles with the produced carbonyl compound to provide an alkenyl oxindole. CeO₂ then receives hydrogen from nano-Ni₂P and hydrogenates the C-3 alkenyl oxindole to give the desired product. Such concerted catalysis by nano-Ni₂P and CeO₂ occurs efficiently, leading to a high catalytic performance in the C-3 alkylation of oxindoles with alcohols. The results of this study also demonstrate that metal phosphides have great potential as highly efficient heterogeneous catalysts, not only in hydrogenation reactions, but also in various other organic syntheses, through concerted effects with metal oxide supports.

Received: 11 February 2021; Accepted: 26 April 2021

Published online: 21 May 2021

References

- Kim, B., Kim, T., Lee, K. & Li, J. Recent advances in transition metal phosphide electrocatalysts for water splitting under neutral pH conditions. *ChemElectroChem* **7**, 3578–3589 (2020).
- Zhang, H. *et al.* Bifunctional heterostructured transition metal phosphides for efficient electrochemical water splitting. *Adv. Funct. Mater.* **30**, 2003261 (2020).
- Weng, C., Ren, J. & Yuan, Z. Transition metal phosphide-based materials for efficient electrochemical hydrogen evolution: A critical review. *ChemSusChem* **13**, 3357–3375 (2020).
- Brock, S. L. & Senevirathne, K. Recent developments in synthetic approaches to transition metal phosphide nanoparticles for magnetic and catalytic application. *J. Solid State Chem.* **181**, 1552–1559 (2008).
- Ren, J. *et al.* Thiophene adsorption and activation on MoP(001), γ -Mo₂N(100), and Ni₂P(001): Density functional theory studies. *J. Phys. Chem. B* **110**, 22563–22569 (2006).
- Sawhill, S. J. *et al.* Thiophene hydrodesulfurization over nickel phosphide catalysts: Effect of the precursor composition and support. *J. Catal.* **231**, 300–313 (2005).
- Liu, P. & Rodriguez, J. A. Catalysts for hydrogen evolution from the [NiFe] hydrogenase to the Ni₂P(001) surface: The importance of ensemble effect. *J. Am. Chem. Soc.* **127**, 14871–14878 (2005).
- Li, K., Wang, R. & Chen, J. Hydrodeoxygenation of anisole over silica-supported Ni₂P, MoP, and NiMoP catalysts. *Energy Fuels* **25**, 854–863 (2011).
- Liu, P., Rodriguez, J. A., Takahashi, Y. & Nakamura, K. Water–gas–shift reaction on a Ni₂P(001) catalyst: Formation of oxyphosphides and highly active reaction sites. *J. Catal.* **262**, 294–303 (2009).
- Liu, P. *et al.* Desulfurization reactions on Ni₂P(001) and α -Mo₂C(001) surfaces: Complex role of P and C sites. *J. Phys. Chem. B* **109**, 4575–4583 (2005).

11. Song, T. *et al.* Highly dispersed single-phase Ni₂P nanoparticles on N, P-codoped porous carbon for efficient synthesis of N-heterocycles. *ACS Sustain. Chem. Eng.* **8**, 267–277 (2020).
12. Feng, H. *et al.* Efficient and sustainable hydrogenation of levulinic acid to gamma-valerolactone in aqueous solution over acid-resistant CePO₄/Co₂P catalysts. *Green Chem.* **21**, 1743–1756 (2019).
13. Sharma, A. K., Joshi, H., Bhaskar, R. & Singh, A. K. Solvent-tailored Pd₃P_{0.95} nano catalyst for amide–nitrile inter-conversion, the hydration of nitriles and transfer hydrogenation of the C=O bond. *Dalton Trans.* **48**, 10962–10970 (2019).
14. Yu, Z. *et al.* Catalytic transfer hydrogenation of levulinic acid to γ-valerolactone over Ni₃P-CePO₄ catalysts. *Ind. Eng. Chem. Res.* **59**, 7416–7425 (2020).
15. Rao, G. K. *et al.* Palladium(II)-1-phenylthio-2-arylchalcogenoethane complexes: Palladium phosphide nano-peanut and ribbon formation controlled by chalcogen and Suzuki coupling activation. *Dalton Trans.* **44**, 6600–6612 (2015).
16. Liu, S. *et al.* Direct synthesis of low-coordinate Pd catalysts supported on SiO₂ via surface organometallic chemistry. *ACS Catal.* **6**, 8380–8388 (2016).
17. Song, T., Ren, P., Xiao, J., Yuan, Y. & Yang, Y. Highly dispersed Ni₂P nanoparticles on N, P-codoped carbon for efficient cross-dehydrogenative coupling to access alkynyl thioethers. *Green Chem.* **22**, 651–656 (2020).
18. Zhao, M. *et al.* Composition-dependent morphology of bi- and trimetallic phosphides: Construction of amorphous Pd-Cu-Ni-P nanoparticles as a selective and versatile catalyst. *ACS Appl. Mater. Interfaces* **9**, 34804–34811 (2017).
19. Fujita, S. *et al.* Unique catalysis of nickel phosphide nanoparticles to promote the selective transformation of biofuranic aldehydes into diketones in water. *ACS Catal.* **10**, 4261–4267 (2020).
20. Gao, R. *et al.* Breaking trade-off between selectivity and activity of nickel-based hydrogenation catalysts by tuning both steric effect and d-band center. *Adv. Sci.* **6**, 1900054 (2019).
21. Wang, H., Shu, Y., Zheng, M. & Zhang, T. Selective hydrogenation of cinnamaldehyde to hydrocinnamaldehyde over SiO₂ supported nickel phosphide catalysts. *Catal. Lett.* **124**, 219–225 (2008).
22. Shi, J. J. *et al.* One-pot synthesized CePO₄/Ni₂P nanocomposites as general hydrogenation catalysts: The attractive contribution of CePO₄. *Appl. Catal. A* **561**, 127–136 (2018).
23. Carencio, S. *et al.* Nickel phosphide nanocatalysts for the chemoselective hydrogenation of alkynes. *Nano Today* **7**, 21–28 (2012).
24. Chen, Y. *et al.* Metal phosphides derived from hydrotalcite precursors toward the selective hydrogenation of phenylacetylene. *ACS Catal.* **5**, 5756–5765 (2015).
25. Albani, D. *et al.* Ensemble design in nickel phosphide catalysts for alkyne semi-hydrogenation. *ChemCatChem* **11**, 457–464 (2019).
26. Zhang, X. *et al.* Naphthalene hydrogenation over silica supported nickel phosphide in the absence and presence of N-containing compounds. *Energy Fuels* **24**, 3796–3803 (2010).
27. Liu, P. *et al.* Mesocellular silica foam supported Ni₂P catalysts with high hydrogenation activity. *React. Kinet. Mech. Catal.* **109**, 105–115 (2013).
28. Bonita, Y., O'Connell, T. P., Miller, H. E. & Hicks, J. C. Revealing the hydrogenation performance of RuMo phosphide for chemoselective reduction of functionalized aromatic hydrocarbons. *Ind. Eng. Chem. Res.* **58**, 3650–3658 (2019).
29. Furukawa, S. *et al.* Remarkable enhancement in hydrogenation ability by phosphidation of ruthenium: Specific surface structure having unique Ru ensembles. *ACS Catal.* **8**, 8177–8181 (2018).
30. Gao, R. *et al.* Ultradispersed nickel phosphide on phosphorus-doped carbon with tailored d-band center for efficient and chemoselective hydrogenation of nitroarenes. *ACS Catal.* **8**, 8420–8429 (2018).
31. Zhu, Y., Yang, S., Cao, C., Song, W. & Wan, L. J. Controllable synthesis of carbon encapsulated iron phosphide nanoparticles for the chemoselective hydrogenation of aromatic nitroarenes to anilines. *Inorg. Chem. Front.* **5**, 1094–1099 (2018).
32. Anutrasakda, W. *et al.* One-pot catalytic conversion of cellobiose to sorbitol over nickel phosphides supported on MCM-41 and Al-MCM-41. *Catalysts* **9**, 92 (2019).
33. Costa, D. C. *et al.* Preparation and characterization of a supported system of Ni₂P/Ni₁₂P₅ nanoparticles and their use as the active phase in chemoselective hydrogenation of acetophenone. *Nanotechnology* **29**, 215702 (2018).
34. Yang, P., Jiang, Z., Ying, P. & Li, C. Effect of surface composition on the catalytic performance of molybdenum phosphide catalysts in the hydrogenation of acetonitrile. *J. Catal.* **253**, 66–73 (2008).
35. Li, X., Zhang, Y., Wang, A., Wang, Y. & Hu, Y. Influence of TiO₂ and CeO₂ on the hydrogenation activity of bulk Ni₂P. *Catal. Commun.* **11**, 1129–1132 (2010).
36. Yu, Z. *et al.* Aqueous phase hydrodeoxygenation of phenol over Ni₃P-CePO₄ catalysts. *Ind. Eng. Chem. Res.* **57**, 10216–10225 (2018).
37. Li, H. & Xu, Y. Liquid phase benzene hydrogenation to cyclohexane over modified Ni-P amorphous catalysts. *Mater. Lett.* **51**, 101–107 (2001).
38. Yang, P., Kobayashi, H., Hara, K. & Fukuoka, A. Phase change of nickel phosphide catalysts in the conversion of cellulose into sorbitol. *ChemSusChem* **5**, 920–926 (2012).
39. Ding, L.-N., Wang, A.-Q., Zheng, M.-Y. & Zhang, T. Selective transformation of cellulose into sorbitol by using a bifunctional nickel phosphide catalyst. *ChemSusChem* **3**, 818–821 (2010).
40. Lin, X., Zeng, X., Zhou, R. & Wang, H. Controlled synthesis of nickel phosphide nanoparticles with pure-phase Ni₂P and Ni₁₂P₅ for hydrogenation of nitrobenzene. *React. Kinet. Mech. Catal.* **126**, 453–461 (2019).
41. Liu, P., Chang, W. T., Liang, X. Y., Wang, J. & Li, X. Y. Small amorphous and crystalline Ni-P particles synthesized in glycol for catalytic hydrogenation of nitrobenzene. *Catal. Commun.* **76**, 42–45 (2016).
42. Yang, S. *et al.* MOF-derived cobalt phosphide/carbon nanocubes for selective hydrogenation of nitroarenes to anilines. *Chem. Eur. J.* **24**, 4234–4238 (2018).
43. Fujita, S. *et al.* Nickel phosphide nanoalloy catalyst for the selective deoxygenation of sulfoxides to sulfides under ambient H₂ pressure. *Org. Biomol. Chem.* **18**, 8827–8833 (2020).
44. Fujita, S. *et al.* Ni₂P nanoalloy as an air-stable and versatile hydrogenation catalyst in water: P-alloying strategy for designing smart catalysts. *Chem. Eur. J.* **27**, 4439–4449 (2021).
45. Yamaguchi, S. *et al.* Air-stable and reusable nickel phosphide nanoparticle catalyst for the highly selective hydrogenation of D-glucose to D-sorbitol. *Green Chem.* **23**, 2010–2020 (2021).
46. Mitsudome, T. *et al.* A cobalt phosphide catalyst for the hydrogenation of nitriles. *Chem. Sci.* **11**, 6682–6689 (2020).
47. Ishikawa, H. *et al.* Air-stable and reusable cobalt phosphide nanoalloy catalyst for selective hydrogenation of furfural derivatives. *ACS Catal.* **11**, 750–757 (2021).
48. Kang, T. H. *et al.* Rhynchophylline and isorhynchophylline inhibit NMDA receptors expressed in *Xenopus* oocytes. *Eur. J. Pharmacol.* **455**, 27–34 (2002).
49. Whatmore, J. L. *et al.* Comparative study of isoflavone, quinoxaline and oxindole families of anti-angiogenic agents. *Angiogenesis* **5**, 45–51 (2002).
50. Peddibhotla, S. 3-Substituted-3-hydroxy-2-oxindole, an emerging new scaffold for drug discovery with potential anti-cancer and other biological activities. *Curr. Bioact. Compd.* **5**, 20–38 (2009).
51. Bartocchini, F., Retini, M. & Piersanti, G. C3-Alkylation of indoles and oxindoles by alcohols by means of borrowing hydrogen methodology. *Tetrahedron Lett.* **61**, 151875 (2020).
52. Di Gregorio, G., Mari, M., Bartolucci, S., Bartocchini, F. & Piersanti, G. Divergent reactions of oxindoles with amino alcohols via the borrowing hydrogen process: Oxindole ring opening vs C3 alkylation. *Org. Chem. Front.* **5**, 1622–1627 (2018).

53. Grigg, R., Whitney, S., Sridharan, V., Keep, A. & Derrick, A. Iridium catalysed C-3 alkylation of oxindole with alcohols under solvent free thermal or microwave conditions. *Tetrahedron* **65**, 4375–4383 (2009).
54. Bisht, G. S., Chaudhari, M. B., Gupte, V. S. & Gnanaprakasam, B. Ru-NHC catalyzed domino reaction of carbonyl compounds and alcohols: A short synthesis of donaxaridine. *ACS Omega* **2**, 8234–8252 (2017).
55. Chaudhari, M. B., Bisht, G. S., Kumari, P. & Gnanaprakasam, B. Ruthenium-catalyzed direct α -alkylation of amides using alcohols. *Org. Biomol. Chem.* **14**, 9215–9220 (2016).
56. Wu, Q., Pan, L., Du, G., Zhang, C. & Wang, D. Preparation of pyridyltriazole ruthenium complexes as effective catalysts for the selective alkylation and one-pot C-H hydroxylation of 2-oxindole with alcohols and mechanism exploration. *Org. Chem. Front.* **5**, 2668–2675 (2018).
57. Jensen, T. & Madsen, R. Ruthenium-catalyzed alkylation of oxindole with alcohols. *J. Org. Chem.* **74**, 3990–3992 (2009).
58. Midya, S. P. *et al.* Ni-catalyzed α -alkylation of unactivated amides and esters with alcohols by hydrogen auto-transfer strategy. *ChemSusChem* **11**, 3911–3916 (2018).
59. Sklyaruk, J., Borghs, J. C., El-Sepelgy, O. & Rueping, M. Catalytic C₁ alkylation with methanol and isotope-labeled methanol. *Angew. Chem. Int. Ed.* **58**, 775–779 (2019).
60. PeÇa-Lopez, M., Piehl, P., Elangovan, S., Neumann, H. & Beller, M. Manganese-catalyzed hydrogen-autotransfer C-C Bond formation: α -Alkylation of ketones with primary alcohols. *Angew. Chem. Int. Ed.* **55**, 14967–14971 (2016).
61. Dambatta, M. B., Polidano, K., Northey, A. D., Williams, J. M. J. & Morrill, L. C. Iron-catalyzed borrowing hydrogen C-alkylation of oxindoles with alcohols. *ChemSusChem* **12**, 2345–2349 (2019).
62. Polidano, K., Allenm, B. D. W., Williams, J. M. J. & Morrill, L. C. Iron-catalyzed methylation using the borrowing hydrogen approach. *ACS Catal.* **8**, 6440–6445 (2018).
63. Chakraborty, P., Garg, N., Manoury, E., Poli, R. & Sundararaju, B. C-alkylation of various carbonucleophiles with secondary alcohols under Co^{III}-catalysis. *ACS Catal.* **10**, 8023–8031 (2020).
64. Chaudhari, C. *et al.* C-3 alkylation of oxindole with alcohols by Pt/CeO₂ catalyst in additive-free conditions. *Catal. Sci. Technol.* **4**, 1064–1069 (2014).
65. Putra, A. E., Oe, Y. & Ohta, T. Pd/C-Catalyzed alkylation of heterocyclic nucleophiles with alcohols through the “borrowing hydrogen” process. *Eur. J. Org. Chem.* 2015(35), 7799–7805 (2015).
66. Liu, G. *et al.* C-3 alkylation of oxindole with alcohols catalyzed by an indene-functionalized mesoporous iridium catalyst. *Catal. Commun.* **12**, 655–659 (2011).
67. Wenkert, E. & Bringi, N. V. A new procedure for forming carbon-carbon bonds. *J. Am. Chem. Soc.* **80**, 5575–5576 (1958).
68. Volk, B., Mezei, T. & Simig, G. Regioselective catalytic alkylation of *N*-heterocycles in continuous flow. *Synthesis* **5**, 595–597 (2002).
69. Liu, Y. J. *et al.* Overcoming the limitations of directed C-H functionalizations of heterocycles. *Nature* **515**, 389–393 (2014).
70. Rossi, L. M., Vono, L. L. R., Garcia, M. A. S., Faria, T. L. T. & Lopez-Sanchez, J. A. Screening of soluble rhodium nanoparticles as precursor for highly active hydrogenation catalysts: The effect of the stabilizing agents. *Top. Catal.* **56**, 1228–1238 (2013).
71. Hayashi, S., Narita, A., Wasano, T., Tachibana, Y. & Kasuya, K. Production of bio-based 2,5-furan dicarboxylate polyesters: Recent progress and critical aspects in their synthesis and thermal properties. *Eur. Polym. J.* **83**, 202–229 (2016).
72. Shimura, K., Kona, K., Siddiki, S. M. A. H. & Shimizu, K. Self-coupling of secondary alcohols by Ni/CeO₂ catalyst. *Appl. Catal. A* **462–463**, 137–142 (2013).
73. de Souza Monteiro, R., Noronha, F. B., Dieguez, L. C. & Schmal, M. Characterization of PdCeO₂ interaction on alumina support and hydrogenation of 1,3-butadiene. *Appl. Catal. A Gen.* **131**, 89–106 (1995).
74. Serrano-Ruiz, J. C., Sepúlveda-Escribano, A., Rodríguez-Reinoso, F. & Duprez, D. Pt–Sn catalysts supported on highly-dispersed ceria on carbon: Application to citral hydrogenation. *J. Mol. Catal. A Chem.* **268**, 227–234 (2007).
75. Liao, X. *et al.* The catalytic hydrogenation of maleic anhydride on CeO_{2- δ} -supported transition metal catalysts. *Catalysts* **7**, 272 (2017).
76. Tang, Z., Cao, H., Tao, Y., Heeres, H. J. & Pescarmona, P. P. Transfer hydrogenation from glycerol over a Ni-Co/CeO₂ catalyst: A highly efficient and sustainable route to produce lactic acid. *Appl. Catal. B Environ.* **263**, 118273 (2020).

Acknowledgements

We thank Dr. Toshiaki Ina (SPring-8) for carrying out the XAFS measurements (2019B1560, 2020A1487 and 2020A1640).

Author contributions

The manuscript was written through the contributions of all authors. All authors have given approval to the final version of the manuscript.

Funding

This work was supported by the Japan Society for the Promotion of Science (JSPS) KAKENHI Grant Nos. 17H03457, 18H01790, and 20H02523. This study was partially supported by the Cooperative Research Program of Institute for Catalysis, Hokkaido University (20B1027) and the Nanotechnology Open Facilities in Osaka University (A-20-OS-0025) of the Ministry of Education, Culture, Sports, Science and Technology (MEXT), Japan.

Competing interests

The authors declare no competing interests.

Additional information

Supplementary Information The online version contains supplementary material available at <https://doi.org/10.1038/s41598-021-89561-1>.

Correspondence and requests for materials should be addressed to T.M.

Reprints and permissions information is available at www.nature.com/reprints.

Publisher's note Springer Nature remains neutral with regard to jurisdictional claims in published maps and institutional affiliations.



Open Access This article is licensed under a Creative Commons Attribution 4.0 International License, which permits use, sharing, adaptation, distribution and reproduction in any medium or format, as long as you give appropriate credit to the original author(s) and the source, provide a link to the Creative Commons licence, and indicate if changes were made. The images or other third party material in this article are included in the article's Creative Commons licence, unless indicated otherwise in a credit line to the material. If material is not included in the article's Creative Commons licence and your intended use is not permitted by statutory regulation or exceeds the permitted use, you will need to obtain permission directly from the copyright holder. To view a copy of this licence, visit <http://creativecommons.org/licenses/by/4.0/>.

© The Author(s) 2021